

PHY2506

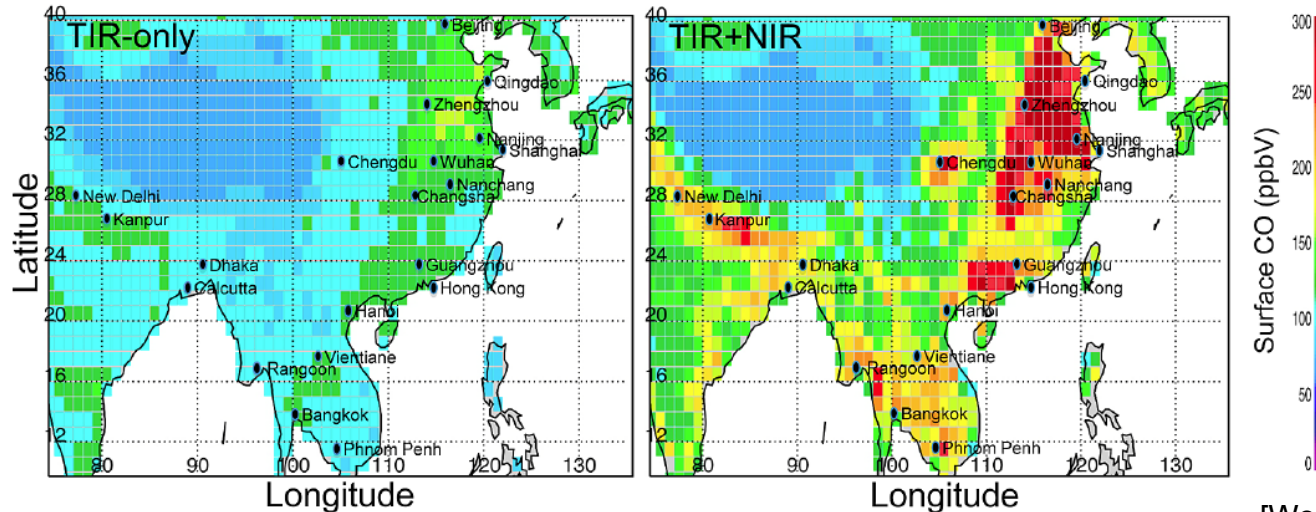
Atmospheric Data Assimilation

Lecture 6

Supplementary Slides

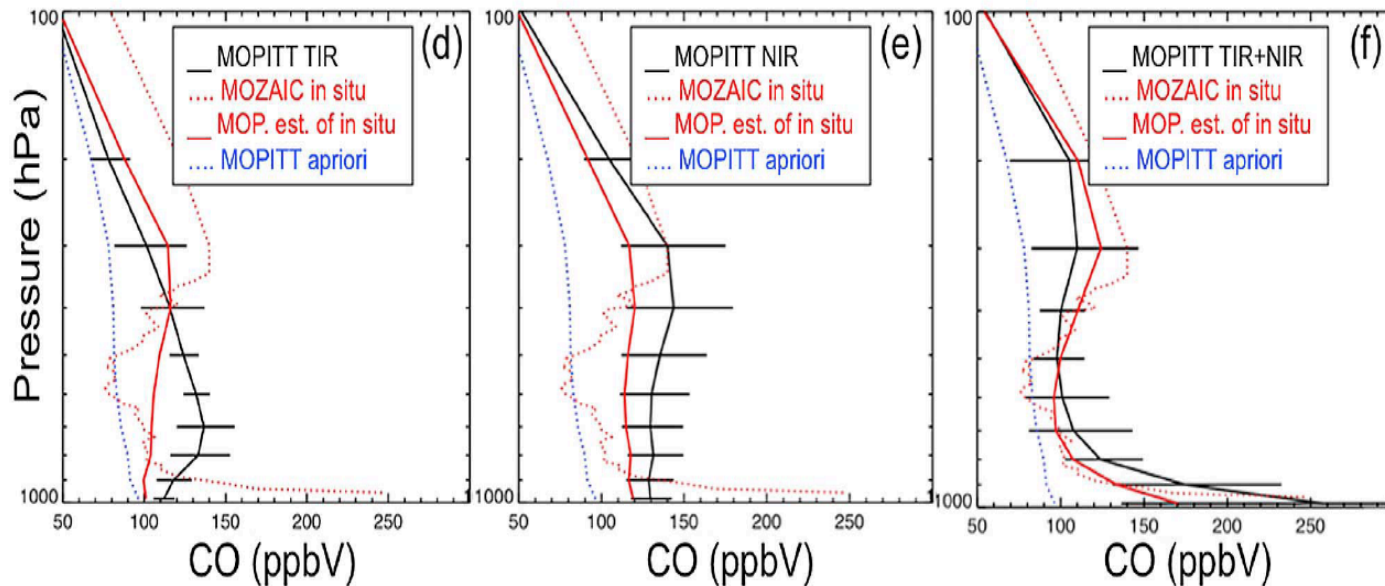
MOPITT Near infrared and thermal infrared retrievals

Mean surface level CO from MOPITT averaged for Sept – Nov, 2004 – 2008



[Worden et al., JGR, 2010]

Comparison of mean MOPITT and MOZAIC profile over New Delhi, India, on 3 Sept. 2004



Version 5 of the MOPITT retrievals provide a good estimate of the CO profile over land

Error Analysis for TES CO Retrievals

D09308

WORDEN ET AL.: PREDICTED ERRORS OF TES NADIR RETRIEVALS

D09308

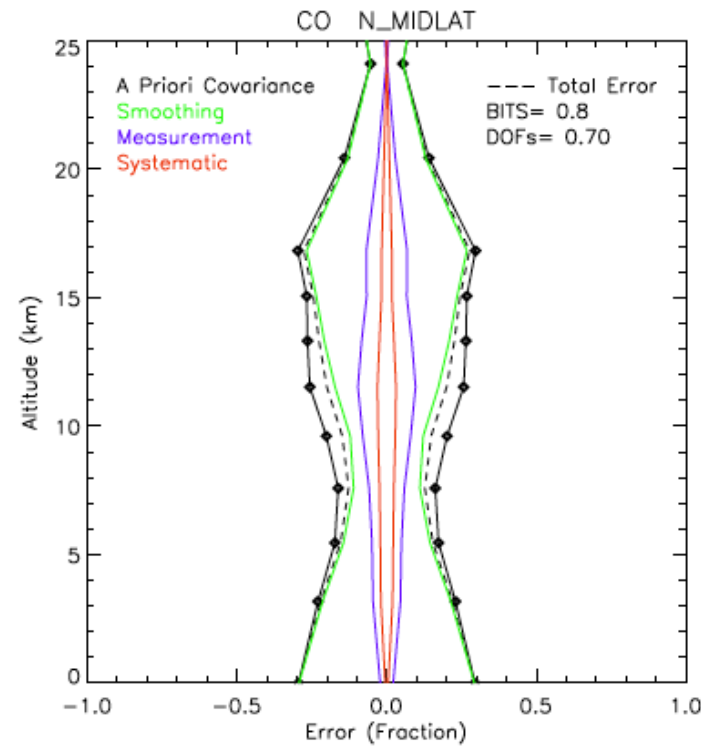
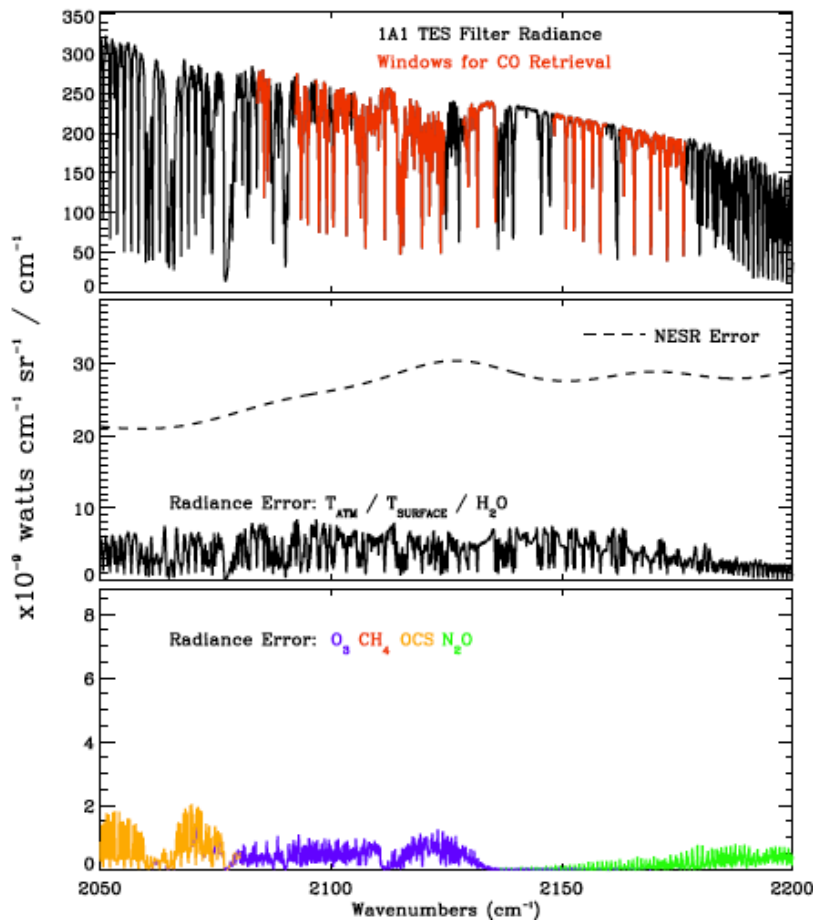


Figure 8. Estimated errors for northern midlatitude CO retrieval using selected spectral windows shown in Figure 7.

Error Analysis for TES O₃ Retrievals

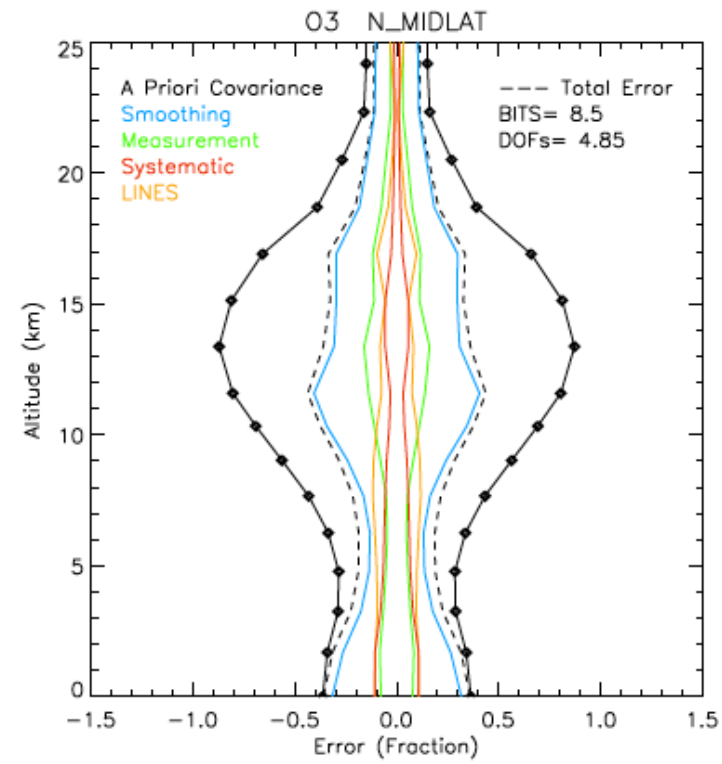
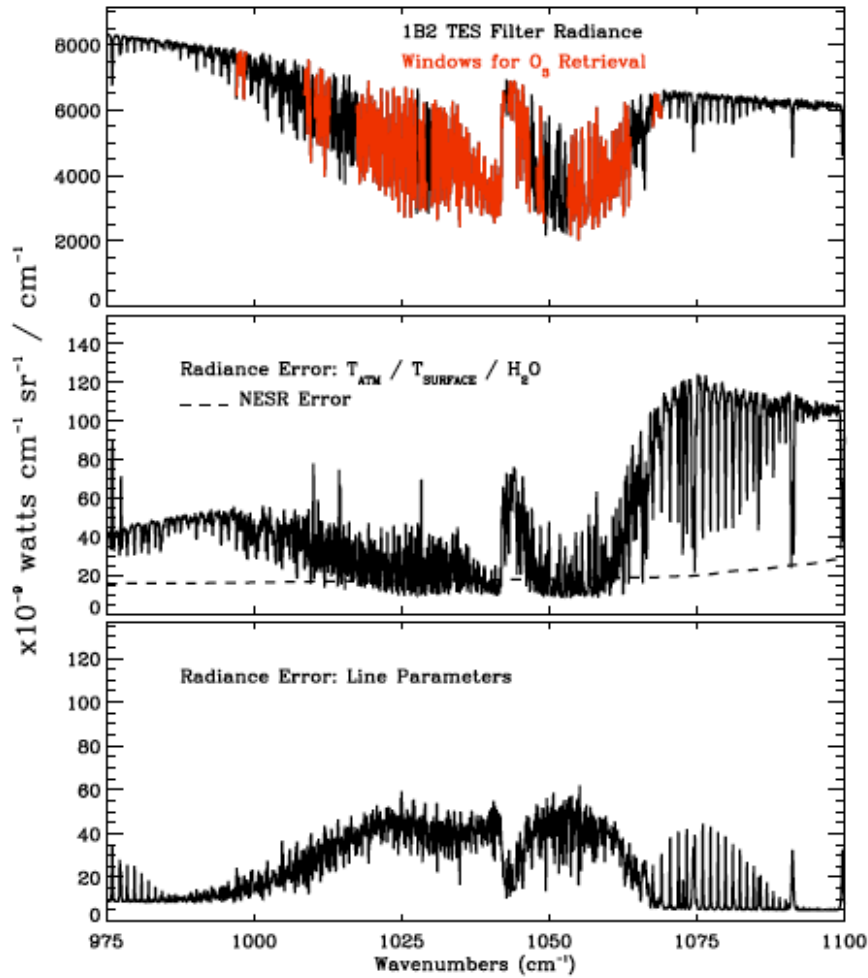


Figure 6. Estimated errors for northern midlatitude O₃ retrieval using selected spectral windows shown in Figure 5. The initial climatological variability is shown with the solid black line, and the a posteriori (total) error is shown with the dashed line. Total error is composed of smoothing error (blue), measurement error (green), systematic errors from H₂O and atmospheric and surface temperature (red), and line parameter errors (orange).

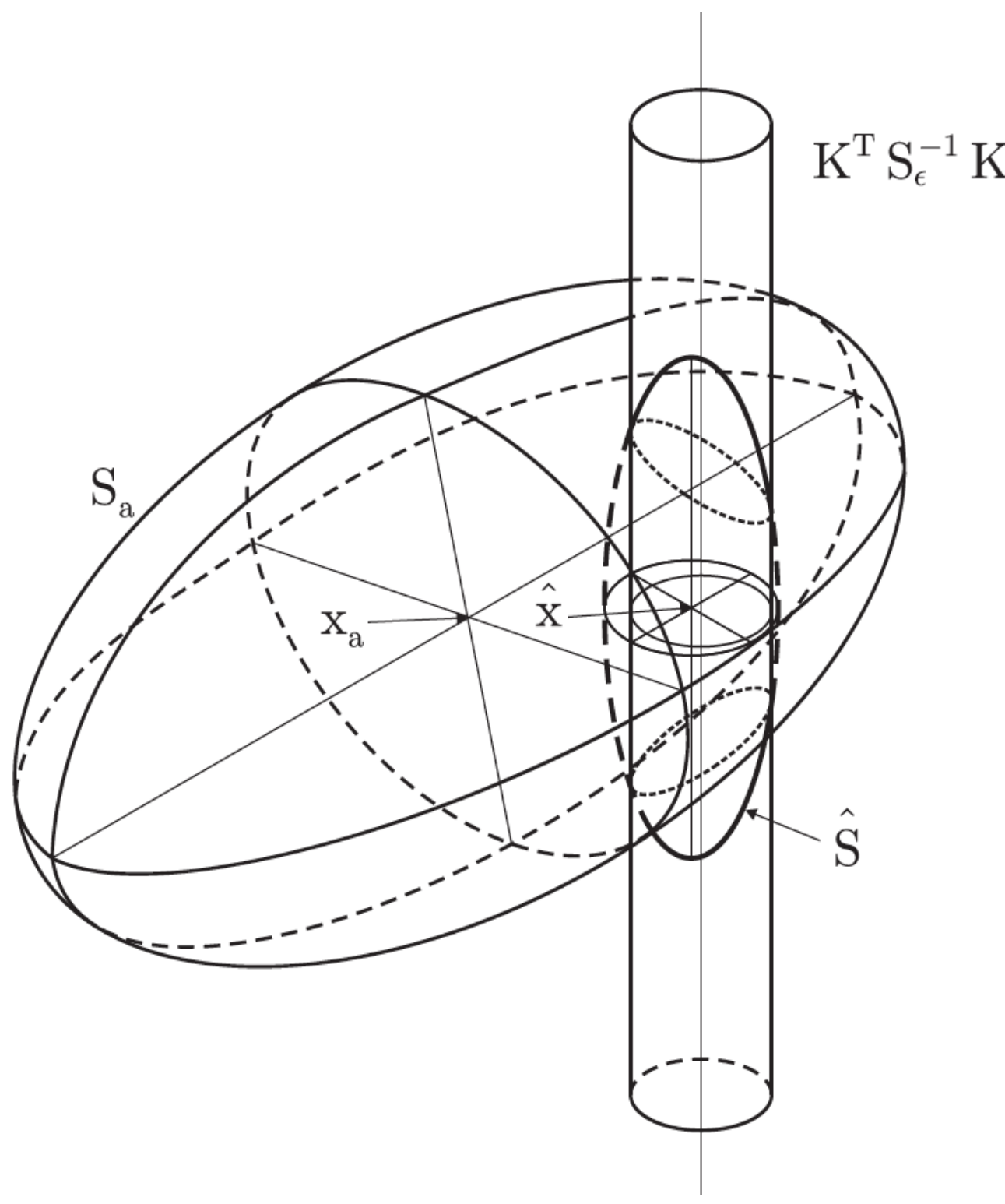


Fig. 2.4 Illustrating the relationship between the prior state estimate, the measurement mapped into state space, and the posterior estimate, for a three-dimensional state space and a two-dimensional measurement space. The large ellipsoid is a contour of the prior *pdf*, the cylinder is a contour of the *pdf* of the state given only the measurement, and the small ellipsoid is a contour of the posterior *pdf*.

[Rodgers, 2000]

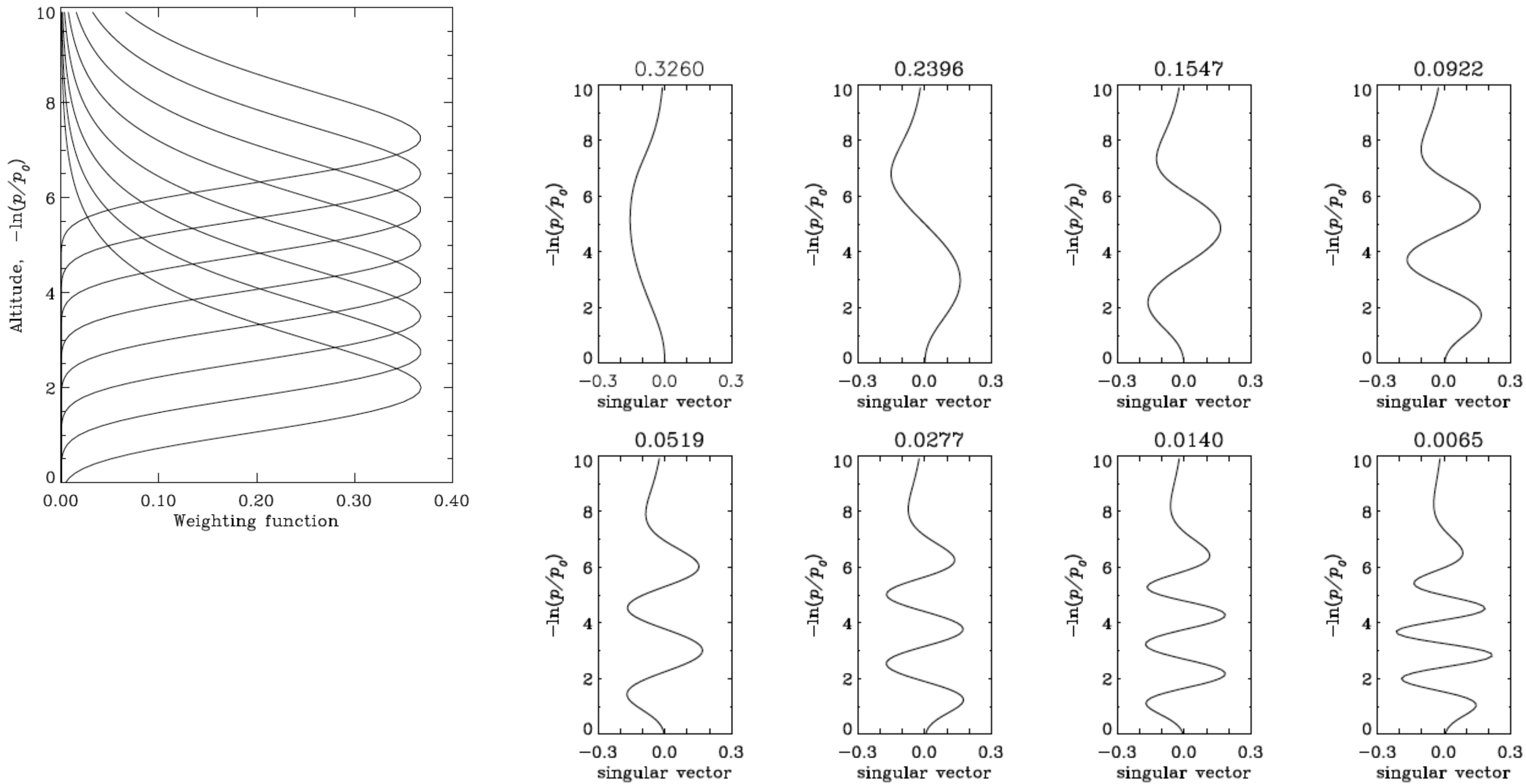


Fig. 2.2 The singular vectors of the weighting functions of Figure 1.1. The corresponding singular values are given above each panel.

[Rodgers, 2000]

Table 2.1 Singular values of $\tilde{\mathbf{K}}$, together with contributions of each vector to the degrees of freedom d_s and information content H for both covariance matrices. Measurement noise variance is 0.25 K^2 .

Diagonal covariance				Full covariance		
i	λ_i	d_{si}	H_i (bits)	λ_i	d_{si}	H_i (bits)
1	6.51929	0.97701	2.72149	27.81364	0.99871	4.79865
2	4.79231	0.95827	2.29147	18.07567	0.99695	4.17818
3	3.09445	0.90544	1.70134	9.94379	0.98999	3.32105
4	1.84370	0.77269	1.06862	5.00738	0.96165	2.35227
5	1.03787	0.51858	0.52731	2.39204	0.85123	1.37443
6	0.55497	0.23547	0.19368	1.09086	0.54337	0.56546
7	0.27941	0.07242	0.05423	0.46770	0.17948	0.14270
8	0.13011	0.01665	0.01211	0.17989	0.03135	0.02297
totals		4.45653	8.57024		5.55272	16.75571

$$S_{ij} = \sigma_a^2 \exp\left(-|i-j|\frac{\delta z}{h}\right) \quad [\text{Rodgers, 2000}] \quad (2.83)$$

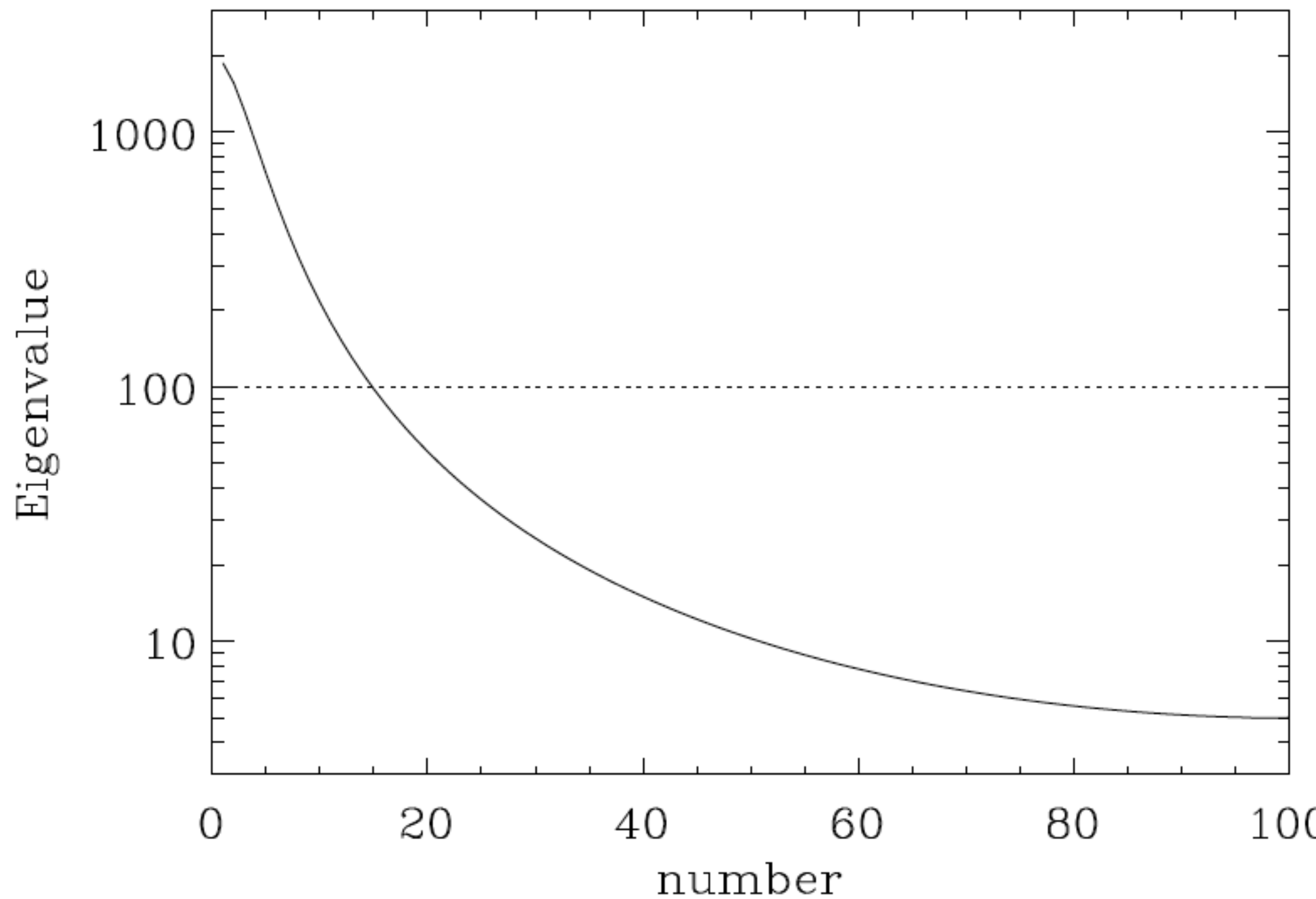


Fig. 2.5 Solid: eigenvalues of a non-diagonal model covariance matrix; dotted: variance of a diagonal covariance matrix with the same total variance.

[Rodgers, 2000]

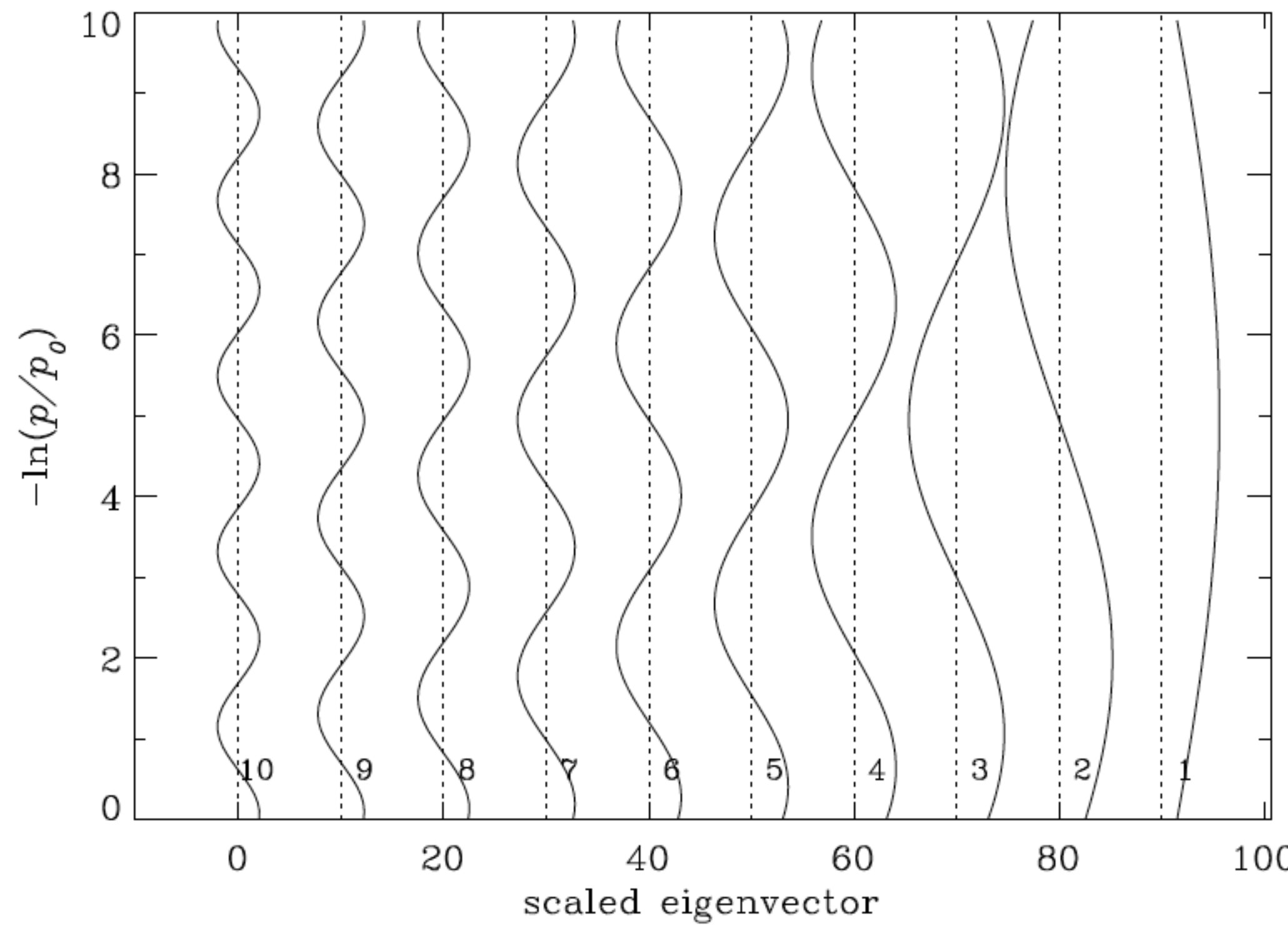


Fig. 3.2 The most significant ten error patterns of the *a priori* covariance matrix $S_{ij} = \sigma_a^2 \exp(-|i - j|\delta z/h)$, for $\sigma_a \simeq 3\text{ K}$ and $h = 1$

[Rodgers, 2000]